

Phosphaalkyne-Bridged Clusters: Synthesis, Characterization, and Nonlinear Optical Properties of $\text{Fe}_4\text{Se}_2(\mu\text{-Se}_2\text{PCBu}^\dagger)(\text{CO})_{11}$

Pradeep Mathur,^{*,1} Sanjukta Ghose,¹ Md. Munkir Hossain,¹
C. V. V. Satyanarayana,² Sudeep Banerjee,³ G. Ravindra Kumar,^{*,3}
Peter B. Hitchcock,⁴ and John F. Nixon^{*,4}

Chemistry Department and Regional Sophisticated Instrumentation Center, Indian Institute of Technology, Powai, Bombay 400 076, India, Tata Institute of Fundamental Research, Homi Bhabha Road, Bombay 400 005, India, and The School of Chemistry, Physics and Environmental Science, University of Sussex, Falmer, Brighton BN1 9QJ, U.K.

Received February 11, 1997[®]

The reaction of $\text{Fe}_2(\text{CO})_6(\mu\text{-Se}_2)$ with $\text{Bu}^t\text{C}\equiv\text{P}$ in THF solvent, in the presence of sodium hydride, yields the tetrairon cluster $\text{Fe}_4\text{Se}_2(\mu\text{-Se}_2\text{PCBu}^\dagger)(\text{CO})_{11}$. It has been characterized by IR and ^1H , ^{31}P , and ^{77}Se NMR spectroscopy, and its molecular structure has been established by single-crystal X-ray diffraction methods. The structure can be described as consisting of a bow-tie type Fe_3Se_2 unit, one face of which is capped by an unusual FeSe_2P unit, in which one Se is 3-coordinate and the other 2-coordinate. The second face is capped by a $\text{P}-\text{C}(\text{CH}_3)$ group such that the P atom is bonded to the middle Fe atom of the Fe_3Se_2 bow tie and the C atom is attached to one Fe atom and one Se atom. Nonlinear optical properties of $\text{Fe}_4\text{Se}_2(\mu\text{-Se}_2\text{PCBu}^\dagger)(\text{CO})_{11}$, measured by the Z-scan technique, indicate significant magnitudes for the third-order susceptibility.

Introduction

Incorporation of certain main-group elements as bridging ligands in transition-metal carbonyl clusters has been an area of active research.⁵ The main-group elements provide stability to the cluster framework and can also act as reactive sites toward inorganic and organic moieties.⁶ Addition of alkynes to the chalcogen atoms of $\text{Fe}_2(\text{CO})_6(\mu\text{-EE}')$, (E, E' = S, Se, Te) occurs at room temperature, and complexes of the type $(\text{CO})_6\text{Fe}_2\{\mu\text{-EC}(\text{Ph})=\text{C}(\text{H})\text{E}'\}$ and $\{(\text{CO})_6\text{Fe}_2\}_2\{\mu\text{-EC}(\text{Ph})-\text{C}(\text{H})\text{E}'\}$ have been isolated.⁷ Such additions block the reactive chalcogen sites and enables different types of additions to be carried out, as in the formation of $\text{Cp}_2\text{Mo}_2\text{Fe}_2(\text{CO})_6(\mu_4\text{-Se})(\mu_3\text{-Se})_2$ and its mixed-chalcogenide variations $\text{Cp}_2\text{Mo}_2\text{Fe}_2(\text{CO})_6(\mu_4\text{-Te})(\mu_3\text{-E})(\mu_3\text{-E}')$ (E, E' = S, Se, Te).⁸ In view of the known similarity in ligating behavior of alkynes and phosphaalkynes, $\text{RC}\equiv\text{P}$,⁹ we have been interested in the reactions of phosphaalkynes with the chalcogen-bridged metal carbonyl compounds: in particular, the reactive $\text{Fe}_2(\text{CO})_6(\mu\text{-E}_2)$ compounds. In contrast to the facile room-temperature addition of

phenylacetylene to $\text{Fe}(\text{CO})_5(\mu\text{-Se}_2)$, in the presence of sodium acetate, the phosphaalkyne $\text{Bu}^t\text{C}\equiv\text{P}$ does not add to $\text{Fe}_2(\text{CO})_6(\mu\text{-Se}_2)$ under similar conditions. In a previous report we have described the synthesis and structural characterization of the phosphaalkyne-bridged pentairon carbonyl cluster $[\{\text{Fe}_3\text{Se}_2(\text{CO})_8\}(\mu\text{-PCBu}^\dagger)\{\text{Fe}_2\text{Se}(\text{CO})_6\}]$ obtained from the photolysis of a hexane solution containing $\text{Fe}_2(\text{CO})_6(\mu\text{-Se}_2)$ and $\text{Bu}^t\text{C}\equiv\text{P}$.¹⁰ Although the exact mechanism of addition of phenylacetylene to $\text{Fe}_2(\text{CO})_6(\mu\text{-Se}_2)$ has not been established, the presence of sodium acetate in the reaction medium is essential for the formation of $(\text{CO})_6\text{Fe}_2\{\mu\text{-SeC}(\text{Ph})=\text{C}(\text{H})\text{Se}\}$ and $\{(\text{CO})_6\text{Fe}_2\}_2\{\mu\text{-SeC}(\text{Ph})-\text{C}(\text{H})\text{Se}\}$. In this paper, we describe the reaction of $\text{Bu}^t\text{C}\equiv\text{P}$ with $\text{Fe}_2(\text{CO})_6(\mu\text{-Se}_2)$ in the presence of sodium hydride and formation of an unusual phosphaalkyne-bridged Fe_4Se_4 cluster.

Clusters are attracting a great deal of attention from researchers in nonlinear optics, because many of them have shown large third-order nonlinearities. There is also the promise of altering the structure of these clusters to obtain better nonlinear optical response. The current focus is on finding materials with a large nonresonant nonlinear response.¹¹ In the search for better nonlinear media for the process of optical limiting,¹² some clusters have been investigated. For instance, C_{60} was shown to be a good optical limiting material. Recently the nonlinear optical properties of some inorganic clusters have been studied, and it was shown that they display significant nonlinearities. We have initiated studies to explore optical nonlinearity in

[®] Abstract published in *Advance ACS Abstracts*, July 15, 1997.

(1) Chemistry Department, Indian Institute of Technology.
(2) Regional Sophisticated Instrumentation Center, Indian Institute of Technology.
(3) Tata Institute of Fundamental Research.
(4) University of Sussex.
(5) (a) Whitmire, K. H. *J. Coord. Chem.* **1988**, *17*, 95. (b) Roof, L. C.; Kolis, J. W. *Chem. Rev.* **1993**, *93*, 1037. (c) Ansari, M. A.; Ibers, J. A. *Coord. Chem. Rev.* **1990**, *100*, 223. (d) Compton, N. A.; Errington, R. J.; Norman, N. C. *Adv. Organomet. Chem.* **1990**, *31*, 91.
(6) Mathur, P.; Chakrabarty, D.; Mavunkal, I. J. *J. Cluster Sci.* **1993**, *4*, 351.
(7) (a) Mathur, P.; Dash, A. K.; Hossain, M. M.; Umbarkar, S.; Satyanarayana, C. V. V.; Chen, Y.-S.; Holt, E.; Rao, S. N.; Soriano, M. *Organometallics* **1996**, *15*, 1356. (b) Mathur, P.; Hossain, M. M.; Umbarkar, S.; Satyanarayana, C. V. V.; Tavale, S. S.; Puranik, V. G. *Organometallics* **1995**, *14*, 959.
(8) Mathur, P.; Hossain, M. M.; Rheingold, A. L. *Organometallics* **1993**, *12*, 5029.
(9) (a) Nixon, J. F. *Chem. Rev.* **1988**, *88*, 1327. (b) *Chem. Ind.* **1993**, 404.

(10) Mathur, P.; Hossain, M. M.; Hitchcock, P. B.; Nixon, J. F. *Organometallics* **1995**, *14*, 3101.

(11) (a) Marder, S. R.; Sohn, J. E.; Stucky, G. D., Eds. *Materials for Nonlinear Optics-Chemical Perspectives*; ACS Symposium Series 455; American Chemical Society: Washington DC, 1991. (b) Bredas, J.-L.; Adant, C.; Tackx, P.; Persoons, A.; Pierce, B. M. *Chem. Rev.* **1994**, *94*, 243.

(12) Tutt, L. W.; Boggess, T. F. *Prog. Quantum Electron.* **1993**, *17*, 299.

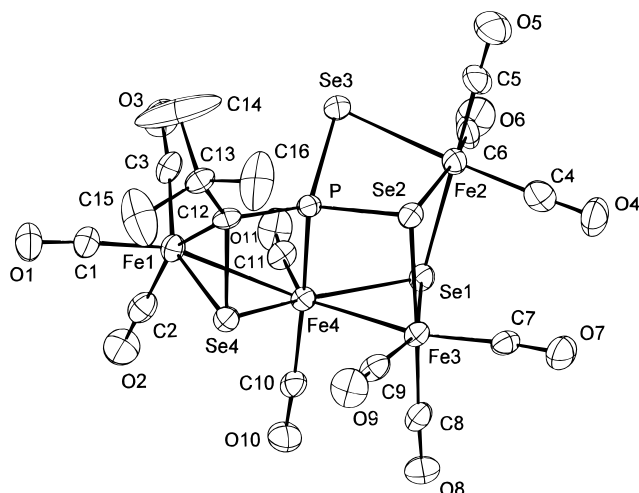


Figure 1. Molecular structure of $\text{Fe}_4\text{Se}_2(\mu\text{-Se}_2\text{PCBu})(\text{CO})_{11}$.

a class of transition-metal, non-metal clusters and have just demonstrated that the nonlinearity in these clusters can far exceed that of C_{60} .¹³ In this paper, we show by measuring the real and imaginary parts of the third-order susceptibility, $\chi^{(3)}$, that the present cluster displays significant nonlinearity. It is also shown that the imaginary part of $\chi^{(3)}$ which leads to nonlinear absorption is significantly larger than those of the compounds $\text{Fe}_2\text{Se}_2(\text{CO})_6$ and $\text{Fe}_3\text{Se}_2(\text{CO})_9$.

Results and Discussion

Synthesis and Characterization. When a mixture of $\text{Fe}_2(\text{CO})_6\text{Se}_2$ and $\text{Bu}^t\text{C}\equiv\text{P}$ in THF solution containing sodium hydride was stirred at room temperature, a single product was isolated and identified as $\text{Fe}_4\text{Se}_2(\mu\text{-Se}_2\text{PCBu})(\text{CO})_{11}$, on the basis of IR and ^1H , ^{31}P , and ^{77}Se NMR spectroscopy. Its composition was confirmed by elemental analysis, and its molecular structure was established by single-crystal X-ray diffraction methods (Figure 1). The crystal data and refinement details are summarized in Table 1, and the selected bond lengths and bond angles are given in Table 2. The IR spectrum revealed the presence of only terminally bonded carbonyl ligands, and the ^1H NMR spectrum showed a single peak for the Bu^t protons. The ^{31}P NMR spectrum showed a single signal with four pairs of P–Se couplings ranging from 31.6 to 360.1 Hz. The ^{77}Se NMR spectrum showed four signals for the different Se atoms, each split into a doublet due to Se–P coupling, the coupling constants being consistent with that observed in the ^{31}P NMR spectrum. The molecular structure of $\text{Fe}_4\text{Se}_2(\mu\text{-Se}_2\text{PCBu})(\text{CO})_{11}$ can be described as consisting of a bow-tie type Fe_3Se_2 unit ($\text{Fe}(1)\text{--Fe}(4)\text{--Fe}(3) = 139.29(7)^\circ$ and $\text{Se}(1)\text{--Fe}(4)\text{--Se}(4) = 143.12(8)^\circ$), one face of which is capped by an unusual FeSe_2P unit, in which one Se is 3-coordinate and the other 2-coordinate. The second face is capped by a P–C(CH₃) group such that the P atom is bonded to the middle Fe atom of the Fe_3Se_2 bow tie and the C atom is attached to one Fe atom and one Se atom. Overall, the P atom has a distorted-tetrahedral coordination around it. Although the two Se atoms in the FeSe_2P ring (Se(3) and Se(2)) display different bonding modes, the angles subtended by them are similar ($\text{P--Se}(3)\text{--Fe}(2) = 80.75(9)^\circ$ and $\text{P--Se}(2)\text{--Fe}($

Table 1. Crystal Data and Structure Refinement for $\text{Fe}_4\text{Se}_2(\mu\text{-Se}_2\text{PCBu})(\text{CO})_{11}$

empirical formula	$\text{C}_{16}\text{H}_9\text{Fe}_4\text{O}_{11}\text{PSe}_4$
fw	947.4
wavelength, Å	0.710 73
<i>a</i> , Å	13.806(10)
<i>b</i> , Å	23.859(17)
<i>c</i> , Å	16.075(11)
α , deg	90
β , deg	90
γ , deg	90
<i>V</i> , Å ³	5295(7)
ρ_{calcd} , Mg m ⁻³	2.38
<i>Z</i>	8
max shift/esd	0.009
abs cor from ψ scans	$T_{\text{max}} = 1.00$, $T_{\text{min}} = 0.39$
abs coeff, mm ⁻¹	7.76
<i>F</i> (000)	3584
θ range, deg	2–25
index ranges	$0 \leq h \leq 16$ $0 \leq k \leq 28$ $0 \leq l \leq 19$
no. of data/restraints/params	4673/0/325
goodness of fit on F^2	1.047
final <i>R</i> indices ($I > 2\sigma(I)$)	$R1 = 0.054$, $wR2 = 0.097$
<i>R</i> (all data)	$R1 = 0.116$, $wR2 = 0.118$
large diff peak/hole, e Å ⁻³	+0.62/−0.80

Table 2. Selected Bond Lengths (Å) and Angles (deg) for $\text{Fe}_4\text{Se}_2(\mu\text{-Se}_2\text{PCBu})(\text{CO})_{11}$

Se(1)–Fe(3)	2.347(2)	Se(4)–C(12)	1.947(9)
Se(1)–Fe(2)	2.507(2)	Se(4)–Fe(1)	2.288(2)
Se(1)–Fe(4)	2.369(2)	Se(4)–Fe(4)	2.388(3)
Se(2)–Fe(2)	2.445(3)	Se(4)–P	2.749(3)
Se(2)–Fe(3)	2.447(2)	Fe(1)–Fe(4)	2.708(2)
Se(2)–P	2.285(3)	Fe(3)–Fe(4)	2.736(2)
Se(3)–P	2.184(3)	Fe(4)–P	2.173(3)
Se(3)–Fe(2)	2.482(2)	P–C(12)	1.781(9)
C(12)–C(13)	1.549(12)		
Fe(3)–Se(1)–Fe(4)	70.91(8)	C(12)–Se(4)–Fe(4)	85.4(2)
Fe(3)–Se(1)–Fe(2)	95.55(6)	C(12)–Se(4)–P	40.2(3)
Fe(4)–Se(1)–Fe(2)	107.20(7)	C(12)–Se(4)–Fe(1)	58.0(3)
Fe(4)–Se(4)–P	49.44(7)	C(12)–Fe(1)–Se(4)	52.7(2)
Fe(2)–Se(2)–Fe(3)	94.66(7)	C(12)–Fe(1)–Fe(4)	75.0(3)
Fe(1)–Se(4)–Fe(4)	70.75(6)	C(12)–P–Fe(4)	96.3(3)
Fe(1)–Se(4)–P	68.51(7)	C(12)–P–Se(3)	121.5(3)
P–Se(2)–Fe(2)	79.63(8)	C(12)–P–Se(2)	120.1(3)
P–Se(2)–Fe(3)	86.56(9)	C(12)–P–Se(4)	44.9(3)
P–Se(3)–Fe(2)	80.75(9)	Se(1)–Fe(4)–Fe(1)	148.10(7)
Se(4)–Fe(1)–Fe(4)	56.34(7)	Se(1)–Fe(4)–Fe(3)	54.18(6)
Se(4)–Fe(4)–Fe(1)	52.91(6)	P–Fe(4)–Se(4)	73.97(8)
Se(4)–Fe(4)–Fe(3)	91.29(6)	P–Fe(4)–Fe(1)	70.79(9)
Se(4)–C(12)–Fe(1)	69.3(3)	P–C(12)–Se(4)	94.9(4)
Se(3)–Fe(2)–Se(1)	98.36(7)	P–C(12)–Fe(1)	95.5(4)
Se(3)–P–Se(2)	95.38(11)	P–Fe(4)–Fe(3)	81.92(9)
Se(3)–P–Se(4)	157.17(13)	Fe(4)–P–Se(3)	119.12(13)
Se(2)–Fe(2)–Se(3)	84.28(7)	Fe(4)–P–Se(2)	104.82(12)
Se(2)–Fe(2)–Se(1)	80.67(6)	Fe(1)–Fe(4)–Fe(3)	139.29(7)
Se(2)–Fe(3)–Fe(4)	85.76(7)	Se(4)–C(12)–C(13)	123.9(6)
Se(2)–P–Se(4)	107.42(10)	Fe(1)–C(12)–C(13)	129.6(7)
Se(1)–Fe(3)–Se(2)	83.91(7)	C(12)–C(13)–C(15)	111.6(9)
Se(1)–Fe(3)–Fe(4)	54.91(5)	C(12)–C(13)–C(14)	110.4(9)
Se(1)–Fe(4)–P	87.24(10)	C(12)–C(13)–C(16)	108.9(8)
Se(1)–Fe(4)–Se(4)	143.12(8)	C(14)–C(13)–C(16)	112.7(13)

(2) = 79.63(8)°). Bonding of the P atom to the 2-coordinate Se atom is slightly shorter ($\text{Se}(3)\text{--P} = 2.184(3)$ Å) than to the 3-coordinate Se atom ($\text{Se}(2)\text{--P} = 2.285(3)$ Å). There are several features of the structure of $\text{Fe}_4\text{Se}_2(\mu\text{-Se}_2\text{PCBu})(\text{CO})_{11}$ that deserve comment. The molecule can be considered as a complex of (Bu^tCPSe) , which does not exist in the free state. The formation of a C–Se bond in $\text{Fe}_4\text{Se}_2(\mu\text{-Se}_2\text{PCBu})(\text{CO})_{11}$ is similar to the formation of the C–Se linkage in the previously reported example of a phosphalkyne functioning as a bridging ligand in the Fe/Se carbonyl cluster, $[\{\text{Fe}_3\text{Se}_2(\text{CO})_8\}(\mu\text{-PCBu})\{\text{Fe}_2\text{Se}(\text{CO})_6\}]$,¹⁰ and can be likened

(13) Banerjee, S.; Kumar, G. R.; Mathur, P.; Sekar, P. *Chem. Commun.* **1997**, 299.

to the C–chalcogen bond formations that occur on the addition of acetylenes to $\text{Fe}_2(\text{CO})_6(\mu\text{-EE}')$ to form $(\text{CO})_6\text{-Fe}_2\{\mu\text{-EC(R)=C(H)E}'\}$.⁷ The mechanism of formation of $\text{Fe}_4\text{Se}_2(\mu\text{-Se}_2\text{PCBu}^t)(\text{CO})_{11}$ has not yet been established, but it can be thought to formally involve the coming together of two $\text{Fe}_2(\text{CO})_6\text{Se}_2$ molecules, rearrangement and loss of one carbonyl ligand, cleavage of the Fe–Fe bond of one molecule, and formation of a new Fe–Fe bond to form the triiron part of the bow-tie unit. One can also view the structure as $\text{Bu}'\text{C}\equiv\text{P}$ linking Fe(1) and Fe(2) via an Fe_2Se_4 unit. The compound $(\text{CO})_6\text{Fe}_2(\mu\text{-Se}_2)$ is known to decompose rapidly in solution, and it is possible that $\text{Fe}(\text{CO})_x$ fragments liberated may influence the reactivity of $\text{Bu}'\text{C}\equiv\text{P}$ toward the Fe/Se/CO fragments generated under thermolytic conditions. The role of sodium hydride in the reaction medium is not clear; when it is absent or when a milder base is used, there is no observable reaction between $(\text{CO})_6\text{Fe}_2(\mu\text{-Se}_2)$ and $\text{Bu}'\text{C}\equiv\text{P}$.

Nonlinear Optical Properties. Nonlinear optical properties of $\text{Fe}_4\text{Se}_2(\mu\text{-Se}_2\text{PCBu}^t)(\text{CO})_{11}$ have been studied using the Z-Scan technique.¹⁴ We have obtained the sign and magnitude of the nonlinear contribution to the refractive index which arises from the third-order susceptibility, $\chi^{(3)}$. Far from the focus the intensity is small and the response of the sample lies in the linear regime. As the sample is moved closer to the focus, the intensity becomes larger and the response becomes nonlinear, with the third-order nonlinearity making the dominant contribution. This leads to modification of both the real and imaginary parts of the refractive index given by $n = n_0 + \gamma I$ and $\alpha = \alpha_0 + \beta I$, where n and α are real and imaginary parts of the refractive index, respectively, and n_0 and α_0 are the corresponding zero-field values. γ and β are the coefficients of nonlinear refraction and absorption, respectively, and I is the intensity. To measure γ , which results in nonlinear refraction, an aperture is inserted in the transmitted beam (closed-aperture scan) and a fraction of the light is collected. To measure β , which results in nonlinear absorption, all of the transmitted beam is collected (open-aperture scan) by means of a large-aperture lens. Standard Z-Scan theory is used to obtain γ and β (eqs 1 and 2)

$$\gamma = (\lambda\alpha_0/0.812\pi l)(1/(1 - \exp(-\alpha_0 l)))\Delta T_{p-v} \quad (1)$$

where ΔT_{p-v} is the difference between the peak and valley of the normalized transmittance of the closed-aperture Z-Scan. Using a two-photon model of nonlinear absorption, open aperture transmission is given by

$$T(z) = (1/\pi^{1/2}q(z)) \int_{-\infty}^{\infty} \ln[1 + q(z)] \exp(-\tau^2) d\tau \quad (2a)$$

$$q(z) = \beta I(z)(1 - \exp(-\alpha_0 l))/\alpha_0 \quad (2b)$$

and β is then obtained by numerically fitting the open-aperture transmittance data to the above expression.

The UV–visible absorption spectrum is shown in Figure 2 (curve 1). The absorption spectrum was measured with the sample taken in a 10 mm pathlength quartz cell. There is low absorption in the visible region, and absorption increases as the wavelength progresses into the UV. From the point of view of nonlinear optics

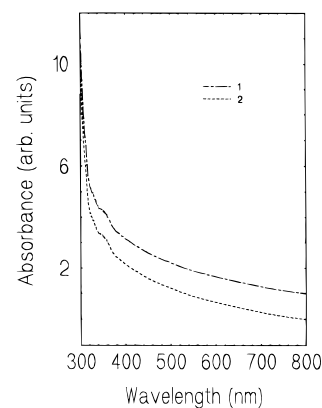


Figure 2. UV–visible absorption spectrum for $\text{Fe}_4\text{Se}_2(\mu\text{-Se}_2\text{PCBu}^t)(\text{CO})_{11}$. Curve 1 shows the spectrum taken before exposure of the sample to an intense laser beam. Curve 2 shows the same after the sample was exposed to the beam for about 3 h.

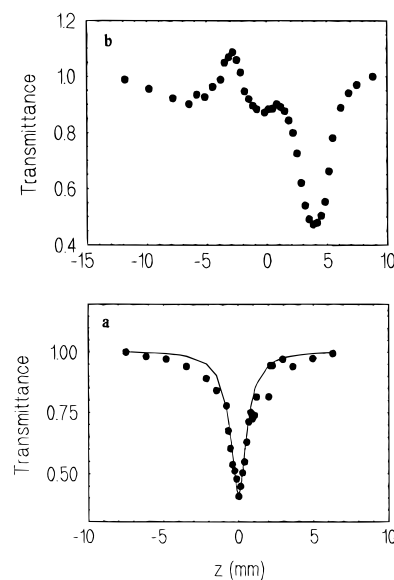


Figure 3. Z-Scan of $\text{Fe}_4\text{Se}_2(\mu\text{-Se}_2\text{PCBu}^t)(\text{CO})_{11}$ at 532 nm: (a) open aperture; (b) closed aperture.

it is interesting to see how the nonlinearity manifests itself in the low-absorption regions, as the response here is mainly expected to come from nonresonant interactions. Our excitation wavelength lies in this region.

Figure 3 shows the results of Z-Scan on this cluster. The open aperture Z-Scan (Figure 3a) shows a large change in transmittance ($>50\%$) indicative of a large absorptive nonlinearity β . By fitting to the expressions given previously (eq 2), one obtains $\beta = 0.8 \times 10^{-7} \text{ cm W}^{-1}$. It is possible that excited-state absorption plays a role in this, but lack of information on the excited states precludes the possibility of making any estimates based on such a picture.

Results of the closed aperture Z-Scan, which depends on the modification of the refractive index, are shown in Figure 3b. The change in transmission is indicative of a defocusing (negative) nonlinearity. The peak to valley difference is about 55%, indicative of considerable nonlinear refraction. The flat portion around focus is possibly due to nonlinear scattering in the sample.¹⁵ Using eq 1 we obtain $\gamma = 1.3 \times 10^{-13} \text{ cm}^2 \text{ W}^{-1}$. The suppression of the peak as indicated by the asymmetry

(14) Sheikh-Bahae, M.; Said, A. A.; Wei, T.-H.; Hagan, D. J.; Van Stryland, E. W. *J. Quantum Electron.* **1990**, *26*, 760.

(15) Chapple, P. B.; Staromlynska, J.; McDuff, R. G. *J. Opt. Soc. Am. B* **1994**, *11*, 975.

Table 3. Comparison of Nonlinear Optical Properties

cluster	α , cm ⁻¹	β , 10 ⁻⁷ cm G W ⁻¹	γ , 10 ⁻¹² cm ² W ⁻¹
Fe ₄ Se ₂ (μ -Se ₂ PCBu [†])(CO) ₁₁	3.8	0.8	1.3
Fe ₂ Se ₂ (CO) ₆	8.9	0.05	0.8
Fe ₃ Se ₂ (CO) ₉	18	0.07	4.5

about the focus can be attributed to the large nonlinear absorption.

To ensure that the sample did not undergo photodegradation as a result of exposure to the intense laser beam, the absorption spectrum was taken after the nonlinear optical measurements were carried out. The absorption spectrum after exposure to the laser beam is shown in Figure 2 (curve 2). It is clear that there is no change in the absorption spectra, and hence photochemical reactions do not contribute to or modify the nonlinear response in any way.

The present cluster compares very well with other NLO materials with regard to both nonlinear refraction and absorption. The value of β is better than other clusters reported recently. The value of γ is of the same order of magnitude as other clusters¹⁶ and exceeds that of C₆₀.¹⁷ We have also compared the nonlinear optical properties of the title cluster with those of Fe₂Se₂(CO)₆ and Fe₃Se₂(CO)₉, which were used in the synthesis. The values are summarized in Table 3. It can be seen that while there is no systematic trend with regard to γ , the value of β is larger, by more than 1 order of magnitude, for Fe₄Se₂(μ -Se₂PCBu[†])(CO)₁₁ as compared to the parent compounds Fe₂Se₂(CO)₆ and Fe₃Se₂(CO)₉. This can be attributed to the greater number of heavy atoms in Fe₄Se₂(μ -Se₂PCBu[†])(CO)₁₁, which introduces more sublevels. The increase in the number of allowed electronic transitions leads to a larger value of $\chi^{(3)}$.¹⁸

Experimental Section

General Procedures. All reactions and other manipulations were carried out using standard Schlenk techniques under an inert atmosphere of argon. All solvents were deoxygenated immediately prior to use. Infrared spectra were recorded on an Impact 400 FTIR spectrophotometer, as hexane solutions in 0.1 mm path length NaCl cells. Elemental analysis was performed using a Carlo-Erba automatic analyzer. ¹H, ⁷⁷Se, and ³¹P NMR spectra were recorded on a Varian VXR-300S spectrometer in CdCl₂. The operating frequency for ⁷⁷Se NMR was 57.23 MHz with a pulse width of 67.5° and a delay of 1 s. Operating frequency for ³¹P NMR was 121.421 MHz, with a pulse width of 45° and a delay of 1 s. The ⁷⁷Se and ³¹P NMR spectra are referenced to Me₂Se (δ 0) and H₃PO₄ (δ 0), respectively. The starting materials Fe₂Se₂(CO)₆¹⁹ and Bu[†]C≡P²⁰ were prepared as reported in the literature.

Reaction of Fe₂Se₂(CO)₆ and Bu[†]C≡P. To a THF solution (50 mL), maintained at 0 °C and containing (CO)₆Fe₂(μ -Se₂) (0.79 g, 1.8 mmol) and sodium hydride (0.17 g, 7.2 mmol), was added Bu[†]C≡P (0.1 mL). The resulting mixture was brought to room temperature and stirred for 24 h. The solution was filtered through Celite to remove insoluble material, and the solvent was removed from the filtrate. The

residue was subjected to chromatographic workup on silica gel TLC plates. Elution with hexane yielded the following compounds, in order of elution: violet (CO)₉Fe₃(μ -Se)₂ (0.08 g, 7%), orange (CO)₆Fe₂(μ -Se₂) (trace amount), and dark brown Fe₄Se₂(μ -Se₂PCBu[†])(CO)₁₁ (0.5 g, 30%). IR: ν (CO) 2084 (s), 2078 (sh), 2061 (vs), 2045 (vs), 2032 (s), 2023 (m), 2011 (vs), 1997 (s), 1986 (s), 1970 (m) cm⁻¹. ¹H NMR: δ 1.17 ppm. ³¹P NMR: δ -4.33 ppm (J_{P-Se} = 360.1, 169.2, 49.4, and 31.6 Hz). ⁷⁷Se NMR: δ 484.6 (d, J_{Se-P} = 49.6 Hz), 385.9 (d, J_{Se-P} = 360.1 Hz), 148.2 (d, J_{Se-P} = 31.3 Hz) and 16.5 (d, J_{Se-P} = 169.4 Hz) ppm. Anal. Calcd for C₁₆H₉Fe₄O₁₁PSe₄: C, 20.2; H, 0.95. Found: C, 20.1; H, 1.01.

X-ray Structure Determination of Fe₄Se₂(μ -Se₂PCBu[†])(CO)₁₁. Dark brown crystals of Fe₄Se₂(μ -Se₂PCBu[†])(CO)₁₁, suitable for X-ray diffraction analysis, were grown from hexane-dichloromethane solvent mixtures by slow evaporation of the solvents at 0 °C. A crystal of approximate dimensions 0.40 × 0.30 × 0.10 mm was used for data collection. Crystallographic data (Table 1) were measured at 293(2) K on a CAD4 automatic four-circle diffractometer, using Enraf-Nonius CAD4 software.²¹ All non-H atoms were anisotropic. Hydrogen atoms were included in the riding mode with $U_{iso}(H)$ equal to 1.2[$U_{eq}(C)$] or 1.5[$U_{eq}(C)$] for methyl groups. A total of 4673 reflections were collected, and 2819 with $I > 2\sigma(I)$ were used in the refinement. Structure analysis was by direct methods, and the refinement was done by full-matrix least-squares procedures. The computing systems used for this were SHELXS-86²² and SHELXL-93,²³ respectively. The interactive graphics and the final drawings were done by CAMERON.²⁴ The crystal system was orthorhombic with a *Pbca* (No. 61) space group.

Study of Nonlinear Optical Properties. The nonlinear optical properties were measured by the Z-scan technique.¹⁴ Light pulses of 35 ps duration at 532 nm from a mode-locked Nd-YAG laser operating at 10 Hz repetition rate were focused by a 20 cm focal length lens into a 1 mm thick quartz cuvette containing the solution of the cluster in *n*-hexane. The cuvette was moved along the axis of the lens by a translation stage. The maximum pulse energy used was 50 nJ, resulting in a peak intensity of 120 MW cm⁻² at the focus spot, whose diameter was measured to be 25 μ m. The linear transmission of the sample was measured to be 67% (low-intensity absorption coefficient α = 3.8 cm⁻¹).

Conclusion

In conclusion, we find that the reaction of the phosphalkyne Bu[†]C≡P with Fe₂(CO)₆(μ -Se₂) occurs in the presence of a strong base to give a phosphalkyne-bridged cluster with an unusual structure. We have measured the third-order nonlinear properties of this cluster and shown that it displays considerable nonlinearity and is a potential optical limiting material.

Acknowledgment. Financial assistance by the Royal Society of Chemistry to P.M. is gratefully acknowledged.

Supporting Information Available: Tables giving details of the X-ray study, atomic coordinates and *B* values, anisotropic displacement parameters, and bond distances and angles (7 pages). Ordering information is given on any current masthead page.

OM9701074

(16) Couris, S.; Koudoumas, E.; Ruth, A. A.; Leach, S. *J. Phys. Chem.* **1995**, *28*, 4537.

(17) Shi, S.; Zhang, X.; Shi, X. F. *J. Phys. Chem.* **1995**, *99*, 14911.

(18) Chen, Z. R.; Hou, H. W.; Xin, X. Q.; Yu, K. B.; Shi, S. *J. Phys. Chem.* **1995**, *99*, 8717.

(19) (a) Mathur, P.; Hossain, M. M. *Organometallics* **1993**, *12*, 2398.

(b) Mathur, P.; Chakrabarty, D.; Hossain, M. M.; Rashid, R. S.; Rugmini, V.; Rheingold, A. L. *Inorg. Chem.* **1992**, *31*, 1106.

(20) Becker, G.; Gresser, G.; Uhl, W. Z. *Naturforsch.* **1981**, *36B*, 16.

(21) Enraf-Nonius CAD4 Software, Version 5.0; Enraf-Nonius, Delft, The Netherlands, 1989.

(22) Sheldrick, G. M. SHELXS-86: Program for the Solution of Crystal Structures; University of Göttingen, Göttingen, Germany, 1985.

(23) Sheldrick, G. M. SHELXL-93: Program for Crystal Structure Refinement; University of Göttingen, Göttingen, Germany, 1985.

(24) Watkin, D. J.; Pearce, L. J. CAMERON: An Interactive Graphics Editor; University of Oxford, Oxford, England, 1993.